Nanotechnology **21** (2010) 165704 (6pp) doi:10.1088/0957-4484/21/16/165704

Nanowire transformation and annealing by Joule heating

Magnus Hummelgård[1], Renyun Zhang[1], Torbjörn Carlberg[1], Damjan Vengust[2], Damjan Dvorsek[2], Dragan Mihailovic[2] and Håkan Olin[1]

[1] Department of Natural Sciences, Engineering and Mathematics, Mid Sweden University, SE-851 70 Sundsvall, Sweden
[2] Jozef Stefan Institute, Jamova 39, SL-1000 Ljubljana, Slovenia

E-mail: magnus.hummelgard@miun.se, dragan.mihailovic@ijs.si and hakan.olin@miun.se

Received 19 October 2009, in final form 2 March 2010
Published 30 March 2010
Online at stacks.iop.org/Nano/21/165704

Abstract
Joule heating of bundles of $Mo_6S_3I_6$ nanowires, in real time, was studied using *in situ* TEM probing. TEM imaging, electron diffraction, and conductivity measurements showed a complete transformation of $Mo_6S_3I_6$ into Mo via thermal decomposition. The resulting Mo nanowires had a conductivity that was 2–3 orders higher than the starting material. The conductivity increased even further, up to 1.8×10^6 S m^{-1}, when the Mo nanowires went through annealing phases. These results suggest that Joule heating might be a general way to transform or anneal nanowires, pointing to applications such as metal nanowire fabrication, novel memory elements based on material transformation, or *in situ* improvement of field emitters.

S Online supplementary data available from stacks.iop.org/Nano/21/165704/mmedia

(Some figures in this article are in colour only in the electronic version)

1. Introduction

Driving a high current through a nanowire leads to increased temperature due to Joule heating. This current induced heating could lead to the failure of nanowires, however, heat could also be used to remove imperfections in the wires by annealing. *In situ* transmission electron microscope (TEM) probing is one method to study these phenomena for direct correlation electrical properties with microstructure of the nanowires during Joule heating. This method employs a tiny scanning tunneling microscope (STM) inside a TEM. The STM tip is used for contacting the nanowire and applying the heating current and at the same time monitoring electrical conductivity, while the TEM is used for imaging of the microstructure.

Such real time *in situ* Joule heating studies have been done on carbon nanotubes, for example, on the transformation of amorphous carbon into crystalline carbon nanotubes [1]. This transformation suggest that the temperature reached is higher than 1700 °C. Joule heating of the carbon nanotubes gives rise to recrystallization with a resulting increase in electrical conductivity [2], or leads to superplastic deformation [3]. Further increasing the electric power eventually leads to breakdown of the wire [4]. *In situ* methods during Joule heating have been used to study other forms of carbon, and graphene sublimation and multi-layer edge reconstruction have been observed [5].

Compound materials are also studied using *in situ* TEM Joule heating, in the form of GaN nanowires and BN nanotubes. *In situ* studies show the thermal decomposition of the GaN nanowires and that Ga nanoparticles separate to the surface of the wire during the failure process [6]. This is of importance since GaN is used in laser diodes operating at high current densities requiring careful consideration of the heat dissipation. Direct *in situ* TEM studies of BN nanotubes show thermal decomposition of tubular layers, leaving spherical nanoparticles behind on the wire surface, before failure [7, 8]. A problem of Joule heating compound nanowires is a positive feedback phenomenon that quickly leads to nanowire failure, due to the decreasing resistance during heating. One way that may prevent this is to limit the current by a serial resistor, preventing a positive feedback, in a way similar to what has been shown in a study of welding of nanowires [9].

Here, we describe a study of a compound nanowire, $Mo_6S_3I_6$, formed as bundles of nanowires [10, 11]. There are a number of applications of these wires, including vapor- and bio-sensors [12], and they can be assembled into more

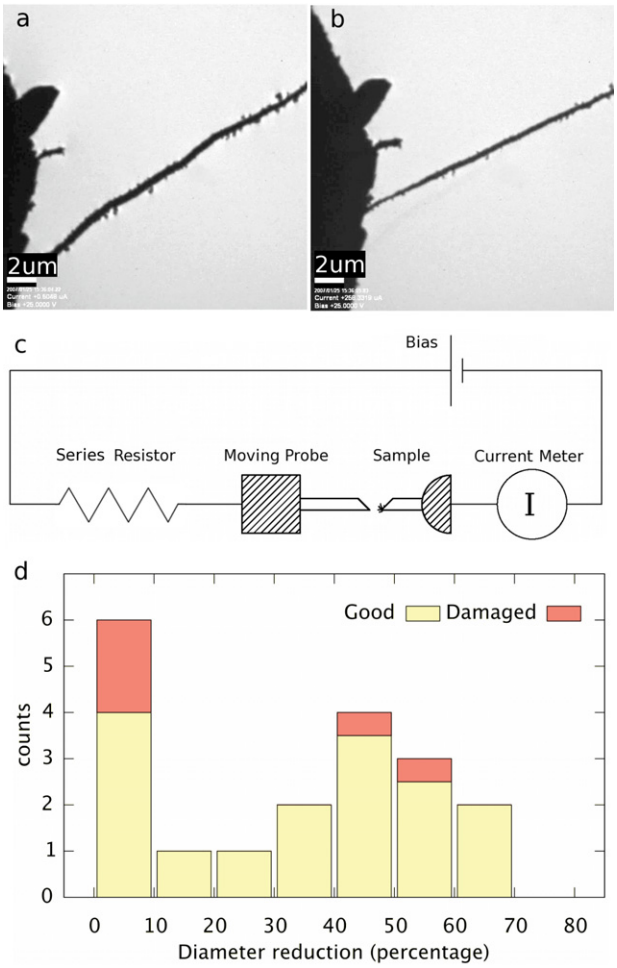

Figure 1. (a) *In situ* TEM image of the $Mo_6S_3I_6$ nanowire bundle before, and (b) after transformation. (c) Diagram of the *in situ* TEM probe. The serial resistor limits the current through the wire bundle. (d) Histogram of the diameter reduction after transformation of $Mo_6S_3I_6$ to Mo.

complex structures [13]. However, the properties during Joule heating are not well known but are of importance in applications such as field emission [14]. We made two main observations: first a transformation of $Mo_6S_3I_6$ to metallic Mo via thermal decomposition. Using a serial resistor to limit the current, allowed us to avoid the nanowire failure until only Mo remained. In the second observation we used these remaining Mo nanowires to study the annealing process, in a way similar to the annealing studies of the carbon nanotubes mentioned above, and reveal details about the grain growth and the increased conductivity.

2. Experimental details

The starting material, $Mo_6S_3I_6$ bundles of nanowires [11], are synthesized in a single-step process and consist of wires with sub-nanometer diameter. During synthesis the nanowires self-assemble into weakly bound bundles. These bundles are easily dispersed in common polar [15] and organic [16] solvents down to individual molecular wires, but here we used the bundles as received (Mo6 company) without further treatment. The electrical conductivity, about 10 S m^{-1}, of these bundles is lower than for metal nanowires [17, 18]. The bundles were 20–1000 nm in diameter and one to several hundred μm in length.

To study the Joule heating process in detail, we carried out experiments on the bundles. This was done inside a transmission electron microscope (JEOL-2000FX) using an *in situ* TEM probe holder [19] (Nanofactory Instruments). In this *in situ* method [20, 21], also called TEM-STM, one electrode is fixed while the other one can be moved in three dimensions by a piezo-electric actuator with sub-nanometer resolution. We used two 0.25 mm gold wires as electrodes, and to attach the bundles to one of them, we simply dipped one of the gold wires in conductive glue and then in the $Mo_6S_3I_6$ material. The two electrodes were connected to an electrical measurement system (figure 1(c)) allowing a current to be passed through the bundles. Inside the TEM, a bundle was selected and moved into contact by the piezo-element. The entire process was observed in real time by TEM imaging or electron diffraction while controlling the current through the wire bundle. Movies of the TEM images or diffraction patterns were recorded, together with corresponding electrical data.

It is hard to measure the temperature of small objects such as nanowires. In the case of semiconducting nanowires, one may use the temperature dependency of current transport through the Schottky barriers that form between the wire and the contacts [7, 8]. Another way is to use a sacrificial material and observe the evaporation of this material during Joule heating. This method has been used on silicon nanowires to estimate the Joule heating temperature by evaporating a thin polymer film previously deposited on the nanowires [22]. Here, we evaporated gold nanoparticles previously deposited on the nanowire bundles. We attached the gold nanoparticles to the surfaces of the bundles in one of the experiments (#15) by mixing them with a solution of sodium citrate followed by sonication, boiling, injection of $HAuCl_4$, and separation by centrifugation [23] (see also details in the supplementary available at stacks.iop.org/Nano/21/165704/mmedia).

3. Results

The first, most apparent, observations were that when increasing the current through the $Mo_6S_3I_6$ bundles, a sudden jump occurred, and the somewhat irregular wires become straight, accompanied by an increase in conductivity by several orders of magnitude (figures 1(a) and (b) and supplementary, movie 1 available at stacks.iop.org/Nano/21/165704/mmedia). During this transformation, the diameters of the $Mo_6S_3I_6$ bundles were reduced by 30–60%, as shown in the histogram in figure 1(d). In addition, electron diffraction clearly showed a transformation of $Mo_6S_3I_6$ to molybdenum (figures 3(d)–(f)).

TEM imaging before and after the transformation and the corresponding conductivity measurements (figure 2) also showed a change in structure of the wires. The fresh $Mo_6S_3I_6$ wire (figure 2, type A) was transformed to an amorphous or polycrystalline wire (type B), with a large increase in conductivity (see the graph in figure 2). After the transformation, by continued heating of the resulting Mo

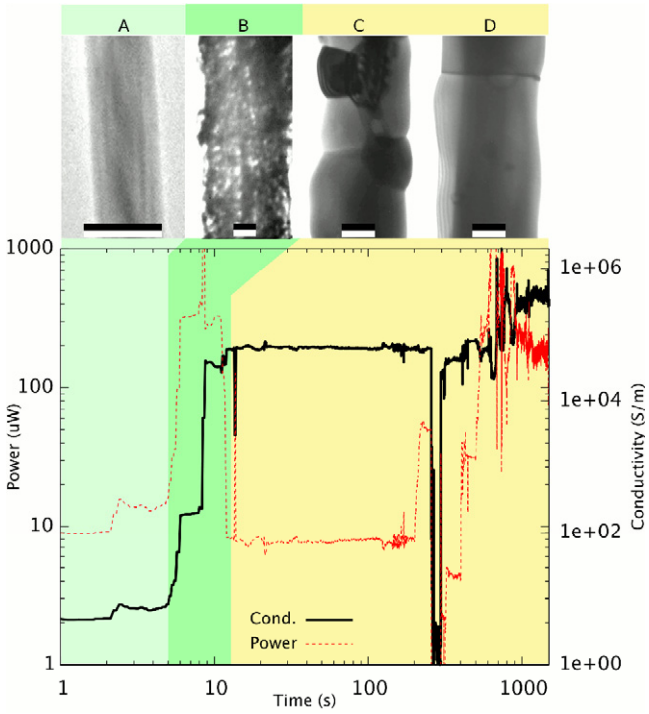

Figure 2. Illustrative TEM images of individual nanowire bundles observed during different stages of current treatment. Note that the images are from several different nanowires. Type A is a fresh sample (scale bar is 100 nm), type B is just after the transformation into a Mo nanowire (scale 50 nm), and type C (scale 50 nm) and D (scale 50 nm) are from the annealing phase. The graph shows the electrical conductivity and the electrical power during the transformation and annealing phases. The conductivity increases in two steps: a fast process during the first few seconds, followed by a slow increase during a longer time. (The drop in current at 300 s is due to a decrease in the bias voltage for diffraction studies.)

nanowire, the small grains in the type B increased into larger ones (type C and D) while the conductivity increased further by 1–2 orders, reaching up to 1.8×10^6 S m^{-1}, which is about one order lower than Mo bulk values (see also the supplementary movie 2 of electron diffraction during the annealing phase available at stacks.iop.org/Nano/21/165704/mmedia). The failure current densities were $>8 \times 10^6$ A cm^{-2} (see table in supplementary available at stacks.iop.org/Nano/21/165704/mmedia). To estimate the annealing temperature, we observed the melting of 50 nm gold nanoparticles in one of the experiment (#15) during the slow annealing phase, which implies a temperature above 1000 °C (figure 4).

4. Discussion

4.1. Transformation via thermal decomposition

The first step, the transformation from $Mo_6S_3I_6$ to metallic Mo, was a fast process, where the structure of the $Mo_6S_3I_6$ wires collapsed as the sulfur and iodine atoms vaporized. The reduction in diameter of 30–60% (figure 2) is consistent with a transformation to metallic molybdenum, since the change in volume will be determined by the ratio of the densities of the two materials which is 5. If we assume that all three dimensions were reduced equally, this amounts to a 40% reduction in diameter, while assuming a fixed length will give a 60% diameter reduction. The expected increase in conductivity of several orders (figure 2), the TEM images (figures 2 and 3), and the electron diffraction (figures 3(d)–(f)) all clearly showed a transformation to Mo.

The transformation can be understood if, in the lack of the ternary system Mo–S–I, the Mo–S phase diagram is studied and if the Mo_2S_3 phase is assumed to be similar to the $Mo_6S_3I_6$ phase with sulfur replacing the iodine atoms. In the temperature range from about 660 to 1550 °C the Mo_2S_3 phase transforms to Mo if sulfur is leaving the lattice. The equilibrium diagram is valid for a gas phase at 1 atm, but in a vacuum, where these experiments were done, it is likely that the volatile constituents can easily leave the lattice, especially as the single wires in the bundles are only about 1 nm in diameter. Upon the collapse, an amorphous structure, or a structure with extremely small crystals form. Heating, up to 900 °C of the $Mo_6S_3I_6$ nanowire bundles in vacuum does not decompose the material, however some signs of iodine evaporation is present above 700 °C [24]. Using the gold melting observation (figure 4) we thus conclude that the transformation temperature was roughly in the range 900–1050 °C.

4.2. Annealing and grain growth

In the next annealing phase, at a temperature above 1000 °C, grain growth occurred. It either started from an amorphous structure with nucleation and growth, or it started with small crystallites which then grew.

Grain growth is often quantitatively treated [25, 26] by the relation

$$D^n - D_0^n = Kt \tag{1}$$

where D is the grain size at a certain time, D_0 is the initial grain size, t is the time and K a constant which depends on the metal composition, temperature and surface energy. The exponent n has been found to vary from 2 to 10 for different cases, but for clean materials at high temperatures the value is close to 2. The process is thermally activated, as it includes atomic diffusion over the grain boundary, and K can be described by an Arrhenius expression.

In the present case an estimation of the growth rate can be done, as it is possible to see when the grains have reached the surface. Equation (1) is only valid as long as the grain growth mainly occurs in the bulk of the wires and as long as only a minority of the grains have reached the surface. It is reasonable to assume that this holds as long as the grains are smaller than about half the diameter of the wires, i.e. at a stage reached somewhat earlier than can be seen in figure 2 type C. From the experiments it can be estimated that the grain size is about 50 nm after about 10 min, which means that the constant K becomes 4×10^{-14} cm^2 s^{-1} if the exponent $n = 2$ is used.

In the literature one can find investigations of grain growth of nanocrystalline materials, e.g. [27] and [28] in Co and W, respectively. In [27], at 530 °C, it was found that the growth deviates from the law represented by equation (1) in such a way that the exponent n changes drastically during the growth

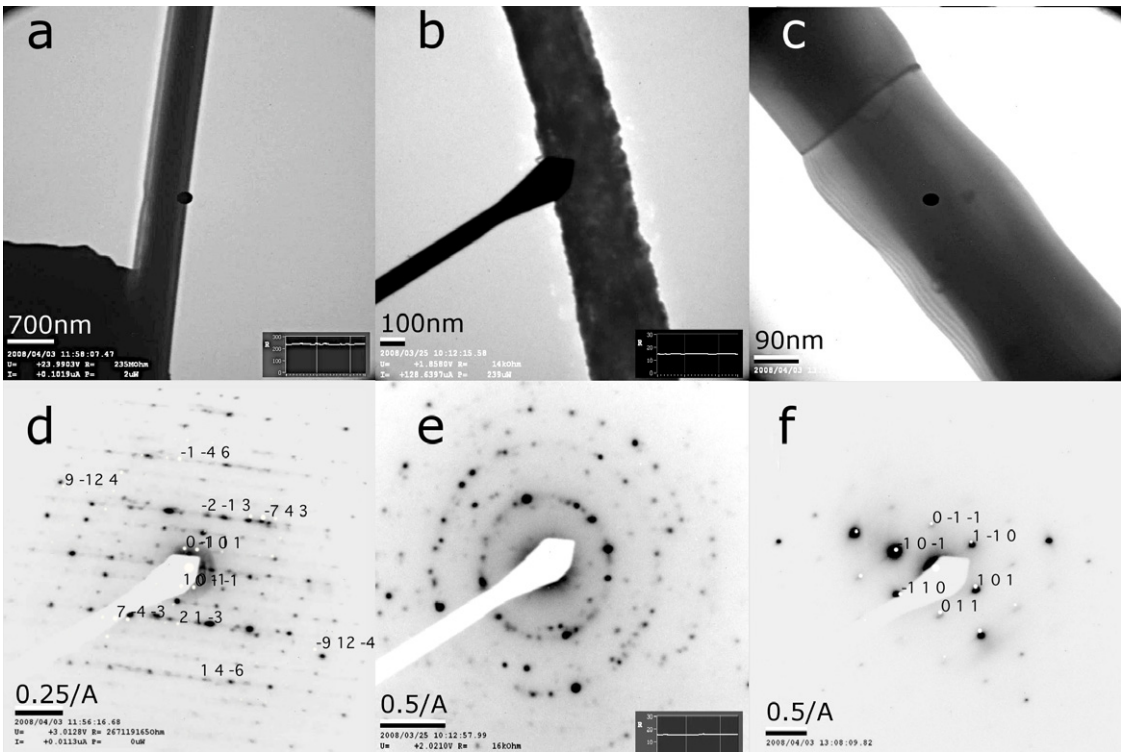

Figure 3. TEM images and diffraction patterns before and after current-heat-treatment of the nanowire bundles. The scale-bars in the images are, respectively, (a) 700 nm, (b) 100 nm, (c) 90 nm, (d) 0.25 $Å^{-1}$, (e) and (f) 0.5 $Å^{-1}$. The black dot in the center of TEM images (a) and (c) is due to an imaging artifact of the TEM. One of the contacts is visible in the bottom-left corner of (a). TEM image (a), with the corresponding electron diffraction pattern indexed to the $Mo_6S_3I_6$ structure (d) is before current treatment. TEM image (b) with the corresponding electron diffraction pattern (e) is the type B structure observed after the nanowire bundle was transformed. TEM image (c) with the corresponding electron diffraction pattern indexed to crystalline Mo (f) shows the resulting type D structure after the slow annealing process. Images (a), (c), (d) and (f) are from the same nanowire while (b) and (e) are from another nanowire.

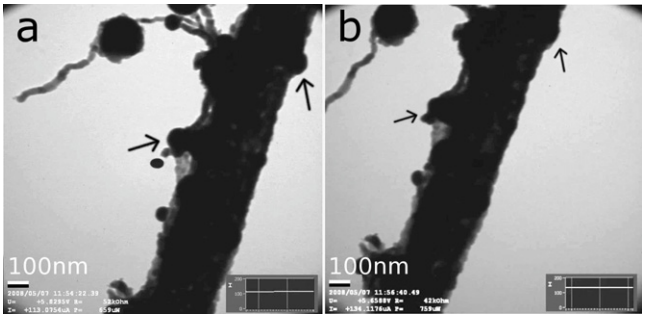

Figure 4. To estimate the temperature, gold nanoparticles (arrowed) were attached to the surfaces, these melted during the slow transformation process, i.e. when the wire changed from type B towards type D. This indicates that the temperature is above ∼1000 °C. TEM images of (a) before melting of gold particles and (b) after. The scale-bar in both TEM images is 100 nm. The black dot in the center of both TEM images is due to a imaging artifact of the TEM.

from about 1.1 to 4.4, and the conclusion was that grain growth in the nano-range is different from in the micro-range. In the present investigation we did not study the grain growth in real time and, therefore, it is not possible to evaluate the exponent as we only have start and end data, but in the part of the data in [27] where the exponent was about 2 the rate constant was about 2×10^{-14} cm^2 s^{-1}, which is fairly close to the value found in the Mo wires. From the data in [28] rate constants, for grain growth in W can be evaluated at different temperatures, and at 1200 °C, which is a third of the melting point, a K value of 2×10^{-14} cm^2 s^{-1} was obtained. A relatively close agreement can thus be found between the present data and the results in the cited investigations if a temperature of about a third of the melting point is chosen for the comparison. It can thus be concluded that grain growth occurs in the Mo wires in a way similar to that previously observed in other nanocrystalline materials.

Depending on the energy balances, and thus the orientation of the grains, the continuing growth rate will be different at different places along the wires. However, data of the pertinent energies indicate that the growth will slow down, or even stop, at many boundaries along the wires, as the surface energy of Mo is about 2 $J\,m^{-2}$ [29] and the grain boundary energy is probably smaller. No data have been found for Mo, but for several other metals the grain boundary energies are given values between 0.5 and 1 $J\,m^{-2}$ [30]. Of course they vary strongly with the type of grain boundary, and at certain points along the wires some grains will shrink and disappear, but the final appearance of the wires, as illustrated in figure 2 type D, is what can be expected.

4.3. Temperature

The gold melting experiment (circa 1000 °C) occurred after the transformation stage and at the beginning of the annealing

phase. This gold melting experiment is similar to the carbon nanotube based method of growing carbon cages by gold templating [31], where the gold evaporates away or intercalates with the carbon nanotube. We might suspect such a mixing of the gold nanoparticles with the Mo nanowire. However, the eutectic temperature of a mixture of Mo–Au is 1054 °C [32], which is close to the melting point of gold, 1064 °C. This means that even if the Au mixes with the Mo nanowire, the temperature estimation from the Au melting/evaporation experiment still gives a valid value. We also know that the temperature was below 2600 °C, at which Mo melts. However, the electrical power during the annealing was well below the failure current when Mo melts, it is thus likely that the temperature was closer to 1000 °C than to the Mo melting point, which is also consistent with the discussion on grain growth above.

In an attempt to correlate the Joule heating current with the temperature, we made a simple model of the wire, following [33], with the contact electrodes as heat sinks and with radiation cooling (see supplementary available at stacks.iop.org/Nano/21/165704/mmedia). However, the resulting temperatures were too high to be realistic. One problem with this approach was the unknown contact resistances. Even if we can calibrate the model using the data from the gold melting experiment, we can not be sure that the contacts were stable over time. We also made current–voltage characterization (see supplementary available at stacks.iop.org/Nano/21/165704/mmedia) showing non-linear relations, that we interpreted as suppressed conductivity at high currents due to phonon-scattering. However, a simple free electron model of this also gave unrealistically high temperatures. One possible source of errors was again the unknown contact resistances.

4.4. Conductivity

It is well known that the conductivities of nanowires are often lower than the corresponding bulk values due to higher degree of scattering at the surface and at the grain boundaries [34–36]. For the smallest, atomic scale nanowires, the electron transport is ballistic, but there is a transition to diffusive transport for larger ones [37]. When the mean free path is longer than the grain size or the diameter of the nanowire, the electron path before scattering will be shortened. The conductivity is proportional to the mean free path and a higher degree of scattering will lead to lower conductivity.

In the present case, we directly observed the grain sizes, and during the annealing phase, the grains coalesce into larger ones that extended throughout the entire nanowire diameter. However, the growth in the axial direction was much slower and we did not extended the study to turn the entire (many micrometer long) nanowire into a single crystal. We thus had a high density of grains, as compared to bulk, with a high degree of scattering at grain boundaries. It is thus not surprising that the conductivity of the Mo nanowire is one order lower than bulk values.

Another source of scattering might be sulfur or iodine atoms left in the wire. However, the solubility of S or I is limited, as can be seen in Mo–S [38] and Mo–I [39] phase diagrams (we lack the ternary diagram Mo–S–I). For example, sulfur does not dissolve in Mo at room temperature and only dissolves at a maximum of 3% at higher temperatures. If there was any S left in the wire at high temperature, it would turn into MoS_2 (with a max of 3% S) when lowering to room temperature. These MoS_2 would then migrate to the surface or to the grain boundaries. We did not specifically study these possible residues, but, at the resolution available in the set-up, no such MoS_2 were visible. EDS, that was not available in the present set-up, might give more information about S or I residuals.

One source of uncertainty in two-terminal conductance measurements is the unknown contact resistances. It is known that the initial contact resistances are high ohmic (MΩ) for *in situ* TEM probing experiments [40], but by driving a high current through the wire the contacts are healed and the resistances decrease. We also observed a similar behavior. In an attempt to model the temperature (see supplementary information available at stacks.iop.org/Nano/21/165704/mmedia) we discussed the role of contact resistance and if we calibrate the temperature model with the gold melting experiments (figure 4) we arrived at initial contact resistances of a few tens of kΩ. However, the contact resistances are still uncertain, and as the resulting Mo nanowires are low ohmic ones, the contacts could constitute a significant part of the resistance. Therefore, instead of subtracting estimated contact resistances, we consider the measured values as a lower limit of the conductivity.

To address this problem of contact resistances, an interesting extension of the present study, that might be possible in a carefully designed set-up, would be to probe the conductivity along the wire and then deduce the nanowire conductivity. If a sharp enough tip is used, for example from another nanowire, it might be possible to directly probe the degree of ballistic transport within each grain and the electron reflection coefficient at the grain boundaries [34].

4.5. Implications for applications

Other molybdenum chalcogenides [41] (Se and Te) have been fabricated in the shape of nanowires with diameters around 1 nm [42] and also occurring as bundles [43]. It is likely that Joule heating of these wires could also result in molybdenum wires, and thus be another route for preparation of molybdenum nanowires. Other metals with high melting temperature such as tungsten, vanadium and niobium, form chalcogenides which decompose at lower temperature, and these metals should also be obtained as nanowires in a similar way. Using the same process it might also be possible to transform conducting metal oxide nanowires [41]. One may also compare the *in situ* Joule heating method with a more standard *in situ* TEM method that utilizes a heating holder. In the standard set-up the temperature is known with a high accuracy. For example, using this kind of heating holder, the thermal decomposition of metal oxides has been studied, such as $W_{18}O_{49}$ [44] as well as annealing of silver wires [45], however, the conductivity data have to be provided *ex situ*.

The high differences in conductivity between fresh wires and metal ones suggest applications as memory

elements [46, 47]. A short pulse of high current would permanently transform a high ohmic nanowire to a low ohmic one, and thus provide two distinct logical states for a kind of nanowire permanent memory. The Joule heating method might also be of general use for improving the crystallinity of nanowires and thus improve the conductivity or mechanical properties. For example, field emitters could be improved by increasing the current to transform or anneal the wires, and indeed this kind of sudden increase in conductivity has already been observed in field emission experiments [14].

5. Conclusion

In conclusion, straight metallic molybdenum nanowires were non-reversibly transformed from $Mo_6S_3I_6$ bundles by Joule heating via thermal decomposition, as consistently observed by the conductivity increase, reduction in diameter, TEM imaging, and electron diffraction. Annealing of the Mo nanowires, with the observed grain growth as result, seems to progress in a way that has been observed in nanocrystalline materials before. Our results suggests that Joule heating might be a general way to anneal or transform nanowires, pointing to applications such as *in situ* improvement of field emitters, metal nanowire fabrication, or novel memory elements based on material transformation.

References

[1] Huang J Y, Chen S, Ren Z F, Chen G and Dresselhaus M S 2006 *Nano Lett.* **6** 1699–705
[2] Chen S, Huang J Y, Wang Z, Kempa K, Chen G and Ren Z F 2005 *Appl. Phys. Lett.* **87** 263107
[3] Huang J Y, Chen S, Wang Z Q, Kempa K, Wang Y M, Jo S H, Chen G, Dresselhaus M S and Ren Z F 2006 *Nature* **439** 281
[4] Huang J Y, Chen S, Jo S H, Wang Z, Han D X, Chen G, Dresselhaus M S and Ren Z F 2005 *Phys. Rev. Lett.* **94** 236802
[5] Huang J Y, Ding F, Yakobson B I, Lu P, Qi L and Li J 2009 *Proc. Natl Acad. Sci. USA* **106** 10103
[6] Westover T, Jones R, Huang J Y, Wang G, Lai E and Talin A A 2009 *Nano Lett.* **9** 257
[7] Xu Z, Golberg D and Bando Y 2009 *Nano Lett.* **9** 2251
[8] Xu Z, Golberg D and Bando Y 2009 *Chem. Phys. Lett.* **480** 110
[9] Tohmyoh H, Imaizumi T, Hayashi H and Saka M 2007 *Scr. Mater.* **57** 953
[10] Vrbanić D *et al* 2004 *Nanotechnology* **15** 635
[11] Mihailovic D 2009 *Prog. Mater. Sci.* **54** 309
[12] Devetak M, Berčič B, Uplaznik M, Mrzel A and Mihailovic D 2008 *Chem. Mater.* **20** 1773
[13] Ploscaru M I, Kokalj S J, Uplaznik M, Vengust D, Turk D, Mrzel A and Mihailovic D 2007 *Nano Lett.* **7** 1445
[14] Zumer M, Nemanic V, Zajec B, Remskar M, Ploscaru M, Vengust D, Mrzel A and Mihailovic D 2005 *Nanotechnology* **16** 1619
[15] Nicolosi V, McCarthy D N, Vengust D, Mihailovic D, Blau W J and Coleman J N 2007 *Eur. Phys. J. Appl. Phys.* **37** 149
[16] McCarthy D N, Nicolosi V, Vengust D, Mihailovic D, Compagnini G, Blau W J and Coleman J N 2007 *J. Appl. Phys.* **101** 014317
[17] Bercic B, Pirnat U, Kusar P, Dvorsek D, Mihailovic D, Vengust D and Podobnik B 2006 *Appl. Phys. Lett.* **88** 173103
[18] Uplaznik M, Bercic B, Strle J, Ploscaru M I, Dvorsek D, Kusar P, Devetak M, Vengust D, Podobnik B and Mihailovic D 2006 *Nanotechnology* **17** 5142
[19] Svensson K, Jompol Y, Olin H and Olsson E 2003 *Rev. Sci. Instrum.* **74** 4945
[20] Erts D, Lohmus A, Lohmus R and Olin H 2001 *Appl. Phys.* A **72** 71
[21] Ziegler K, Lyons D, Holmes J, Erts D, Polyakov B, Olin H, Svensson K and Olsson E 2004 *Appl. Phys. Lett.* **84** 4074
[22] Park I, Li Z, Pisano A P and Williams R S 2007 *Int. Mechanical Engineering Congr. and Exposition (Seattle)* vol 11 (Washington, WA: Amer. Soc. Mech. Engineers) p 1101
[23] Zhang R, Hummelgård M and Olin H 2009 *Mater. Sci. Eng.* B **158** 48
[24] Berčič B, Pirnat U, Kusar P, Dvorsek D, Mihailovic D, Vengust D and Podobnik B 2006 *Appl. Phys. Lett.* **88** 173103
[25] Hillert M 1965 *Acta Metall.* **13** 227
[26] Atkinson H V 1988 *Acta Metall.* **36** 469
[27] Song X, Zhang J, Li L, Yang K and Liu G 2006 *Acta Mater.* **54** 5541–50
[28] Fan J, Huang B, Qu X and Zou Z 2001 *Int. J. Refract. Met. Hard Mater.* **19** 73–7
[29] Lesnik N D, Pestun T S and Eremenko V N 1970 *Poroshk. Metall.* **94** 83–9
[30] Askeland D R 1996 *The Science and Engineering of Materials* 3rd edn (London: Chapman and Hall) p 102
[31] Zhang R, Hummelgård M and Olin H 2009 *Carbon* **48** 424
[32] Massalski T B, Okamoto H and Brewer L 1986 *J. Phase Equilib.* **7** 449
[33] Vincent P, Purcell S T, Journet C and Binh V T 2002 *Phys. Rev.* B **66** 075406
[34] Durkan C and Welland M E 1999 *Phys. Rev.* B **61** 14215
[35] Reiss G, Vancea J and Hoffmann H 1986 *Phys. Rev. Lett.* **56** 2100
[36] Bietsch A and Michel B 2002 *Appl. Phys. Lett.* **80** 3346
[37] Erts D, Olin H, Ryen L, Olsson E and Thölén A 2000 *Phys. Rev.* B **61** 12725
[38] Brewer L and Lamoreaux R H 1980 *J. Phase Equilib.* **1** 93
[39] Brewer L and Lamoreaux R H 1980 *J. Phase Equilib.* **1** 80
[40] Svensson K, Olin H and Olsson E 2004 *Phys. Rev. Lett.* **93** 145901
[41] Xia Y, Yang P, Sun Y, Wu Y, Mayers B, Gates B, Yin Y, Kim F and Yan H 2003 *Adv. Mater.* **15** 353
[42] Venkataraman L and Lieber C M 1999 *Phys. Rev. Lett.* **83** 5334
[43] Golden J H, DiSalvo F J, Frchet J M, Silcox J, Thomas M and Elman J 1996 *Science* **273** 782
[44] Chen C L and Mori H 2009 *Nanotechnology* **20** 285604
[45] Chen C L, Furusho H and Mori H 2009 *Nanotechnology* **20** 405605
[46] Lee S H, Ko D K, Jung Y and Agarwal R 2006 *Appl. Phys. Lett.* **89** 223116
[47] Sivaramakrishnan S, Chia P, Yeo Y, Chua L and Ho P 2007 *Nat. Mater.* **6** 149–55